CHIN. PHYS. LETT. Vol. 27, No. 8 (2010) 086401

Phase Relations and Pressure-Volume-Temperature Equation of State of Galena *

FAN Da-Wei(范大伟)[1], ZHOU Wen-Ge(周文戈)[1**], WEI Shu-Yi(魏舒怡)[1,3], LIU Jing(刘景)[2], LI Yan-Chun(李延春)[2], JIANG Sheng(蒋升)[2], XIE Hong-Sen(谢鸿森)[1]

[1]*Laboratory for Study of the Earth's Interior and Geofluids, Institute of Geochemistry, Chinese Academy of Sciences, Guiyang 550002*

[2]*Institute of High Energy Physics, Chinese Academy of Sciences, Beijing 100049*

[3]*Graduate University of the Chinese Academy of Sciences, Beijing 100049*

(Received 7 April 2010)

The phase relations and pressure volume dependences of galena (PbS) under high pressure and high temperature are investigated by means of in situ observation using resistance heating in a diamond anvil cell and synchrotron radiation. The phase transition from NaCl type to TlI type takes place at approximately 2.4 GPa. A fit to the high temperature third-order Birch–Murnaghan equation of state yields an isothermal bulk modulus $K_0 = 37(3)$ *GPa, and its pressure derivative* $K_0' = 3.6(3)$*, the temperature derivative of the bulk modulus* $(\partial K/\partial T)_P = -0.022(9)$ *GPaK*$^{-1}$*, and the thermal expansion coefficient* $\alpha_0 = 2.2(5) \times 10^{-5}\,K^{-1}$ *for TlI-type galena. The linear compressibilities* β *along a, b and c directions of TlI type is elastically anisotropic (*$\beta_a = 3.4 \times 10^{-3}$ *GPa*$^{-1}$*,* $\beta_b = 1.4 \times 10^{-4}$ *GPa*$^{-1}$ *and* $\beta_c = 1.6 \times 10^{-3}$ *GPa*$^{-1}$*). We obtain the temperature derivative of the bulk modulus* $(\partial K/\partial T)_P$ *and thermal expansion coefficient* α_0 *for TlI-type galena for the first time.*

PACS: 64. 30. Jk, 07. 35. +k, 07. 85. Qe DOI: 10.1088/0256-307X/27/8/086401

Galena (PbS) is one of the most abundant and widely distributed sulfide minerals. The structure of galena is identical to that of halite, NaCl. The two minerals have the same crystal shapes, symmetry and cleavage. Since the equation of state (EOS) enables us to determine the important elastic parameters such as bulk modulus and its pressure derivative, the EOS of substances have been extensively studied at high pressure.[1–5] In addition, the phase relations and EOS of galena (PbS) have also been widely investigated by many methods (resistivity measurement, energy dispersive x-ray powder diffraction and angle dispersive x-ray powder diffraction).[6–12] Samara *et al.*[6] investigated the phase transition of PbS in high pressure by resistivity measurements and have shown that the transition pressure of PbS is about 2.2 GPa. Subsequent researchers[7–12] also found the phase transition of PbS under high pressure. Chattopadhyay *et al.*[7] made high pressure energy dispersive x-ray diffraction study on the structural phase transitions in PbS, PbSe and PbTe using a synchrotron x-ray source. They showed the phase transition in PbS, PbSe and PbTe from rocksalt structure (NaCl type) to orthorhombic structure (TlI type) at 2.2, 4.5 and 6.0 GPa. Knorr *et al.*[8] reported the phase transition (from NaCl type to TlI type) of PbS at 2.5 GPa, and the bulk moduli of NaCl type and TlI type are 51.0 and 30.9 GPa, respectively. Recently, Grzechnik and Friese[9] showed the phase transition of PbS from NaCl type to TlI type at 2.2 GPa by single-crystal x-ray diffraction in a diamond anvil cell. In addition, Ahuja *et al.*[10] investigated the structural behavior of PbS, PbSe and PbTe by means of first principles total energy calculations, and obtained the bulk moduli of PbS, PbSe and PbTe to be 34.0, 31.0, 27.0 GPa, respectively. However, to date, no phase transition and pressure-volume-temperature (PVT) equation of state of PbS has been reported at high pressure and high temperature simultaneously. A detailed study including crystal structure and high-pressure high-temperature unit-cell parameters can provide very important information for understanding the behavior of galena (PbS) at high pressure and temperature. Therefore, in this study, we report the phase transition and the PVT equation of state of galena obtained up to pressures of 19 GPa in the temperature range 300–653 K using resistance heating in a diamond anvil cell and energy dispersive x-ray diffraction radiation.

A natural galena was collected from Gejiu tin deposit, in Yunnan province of China. Chemical composition of the galena was determined by electron probe, and chemical formula of the crystal was calculated to be $Pb_{0.99}S_{1.01}$. The phase of this sample is NaCl type characterized by conventional x-ray diffraction. The sample was ground under acetone in an agate mortar to an average grain size of 5–10 μm and dried.

The *in situ* high-pressure high temperature x-ray energy dispersive diffraction experiments on a galena were carried out with an external resistive heating diamond anvil cell (DAC) at the High Pressure Experiment Station, Beijing Synchrotron Radiation Facility (BSRF). The size of the x-ray spot is 50 μm × 30 μm and the culet of the DAC is 500 μm. The sample powder was loaded with the inner pressure standard Pt powder into a 200-μm hole in a T301 stainless steel gasket. The pressure medium was a mixture of methanol and ethanol and water with 16 : 3 : 1. The pressure in the DAC was calculated according to the

*Supported by the Funds for Huge Scientific Equipment from the National Natural Science Foundation of China and Chinese Academy of Sciences under Grant No 10979053, the Knowledge Innovation Project of Chinese Academy of Sciences (KJCX2-SW-N20) and the National Natural Science Foundation of China under Grant No 40873052, the Guizhou Foundation for Science and Technology under Grant No [2010]2231.

**To whom correspondence should be addressed. Email: wengezhou67@163.com

equation of state of Pt.[13] Heating was carried out using an exterior-heating system, and temperature was measured by a NiCr-NiSi thermocouple in precision of ±2°C. The diffraction angle $2\theta = 14.118° \pm 0.023°$, which was calibrated by diffractive peaks of Pt. Details of the experimental technique have been described in Ref. [14].

Table 1. Cell parameters versus pressure and temperature for galena ($Pb_{0.99}S_{1.01}$). The numbers in parentheses are uncertainties on the last digits.

P (GPa)	T (K)	a (Å)	b (Å)	c (Å)	V (Å^3)
Rocksalt structure					
0.0	300	5.921(1)			207.5(1)
Orthorhombic structure					
2.4	300	4.01(4)	11.25(6)	4.11(3)	185.4(4)
5.8	300	3.90(5)	11.09(4)	4.05(2)	175.1(5)
7.8	300	3.85(3)	10.98(7)	4.02(2)	170.0(4)
9.9	300	3.78(5)	10.85(4)	3.97(6)	162.7(1)
10.8	300	3.75(6)	10.82(6)	3.96(2)	160.8(1)
11.6	300	3.72(4)	10.79(3)	3.95(3)	158.6(3)
14.8	300	3.66(3)	10.67(3)	3.90(3)	152.4(9)
19.0	300	3.60(5)	10.52(6)	3.85(3)	145.9(5)
15.7	373	3.64(4)	10.71(4)	3.91(5)	152.4(6)
13.4	373	3.67(5)	10.73(2)	3.98(4)	156.6(8)
13.0	373	3.68(3)	10.74(3)	3.99(3)	157.7(9)
9.5	373	3.75(2)	10.82(8)	4.08(6)	165.7(5)
14.5	463	3.69(4)	10.75(5)	3.93(8)	156.0(8)
13.7	463	3.71(5)	10.76(4)	3.94(5)	157.4(9)
11.9	463	3.75(3)	10.81(2)	3.98(4)	161.5(4)
10.2	463	3.79(6)	10.86(3)	4.02(5)	165.6(6)
18.0	558	3.61(8)	10.72(5)	3.90(4)	150.8(4)
16.6	558	3.64(7)	10.75(5)	3.92(6)	153.2(8)
13.0	558	3.71(5)	10.81(6)	4.00(7)	160.2(4)
12.1	558	3.73(4)	10.84(7)	4.01(2)	162.2(7)
15.9	653	3.66(5)	10.78(8)	3.95(3)	155.9(6)
13.5	653	3.70(3)	10.82(5)	4.01(8)	160.7(3)
11.1	653	3.76(2)	10.87(6)	4.07(7)	166.3(5)
10.7	653	3.77(5)	10.89(3)	4.06(4)	166.9(7)

Temperature was kept for 600 s before the spectrum was collected. First, we gradually increased the pressure to a highest value in this study (19.0 GPa). Second, the temperature was raised to 653 K gradually, and the spectrum was collected every 100°. Then, we decreased the pressure and repeated the heating and data gathering process. Typical spectra at selected pressures and temperatures are shown in Fig. 1. We read the energy E_{hkl} coupled with every peak by the Maestro software and calculated the distance d_{hkl}(Å) using the energy dispersive formula ($E_{hkl} \times d_{hkl} = 6.199/\sin\theta$). Then, the cell parameters of stibnite were calculated by the unitcell process,[15] as listed Table 1.

X-ray diffraction patterns of galena ($Pb_{0.99}S_{1.01}$) observed in the present study are shown in Fig. 1. These profiles are respective single phases and representative diffraction lines are indexed. Galena is the rocksalt structure at room temperature and atmospheric pressure, and its characteristic diffraction peaks are 200, 220, 311 and 222, respectively (Fig. 1). With the pressure increasing, the transition from the rocksalt structure (NaCl type) to the orthorhombic structure (TlI type) at about 2.4 GPa appears. In this study, the pressure for phase transition from NaCl type to TlI type is the same as the previous studies.[7,8] However, TlI type is only an intermediate phase. Further structural phase transitions from the intermediate phase to the CsCl type phase of PbS appear at about 21.5 GPa.[7] For comparison, the phase transition pressures of PbSe and PbTe transforming from TlI type to CsCl type are 16.0 and 13.0 GPa, respectively.[7] Comparing the phase transition pressures of PbS, PbSe and PbTe from TlI type to CsCl type, we can find that the phase transition pressures reduce in turn with the increasing atomic number in anion. This phenomenon exists not only in lead chalcogenides (PbS, PbSe and PbTe), but also in mercury chalcogenides (HgS, HgSe and HgTe) and zinc chalcogenides (ZnS, ZnSe and ZnTe).[15–20] In addition, Kumar *et al.*[21] and Tinoco *et al.*[22] also showed that the pressure of transformation decreases with the increasing anion radius by the study of the phase transitions for $CuInS_2$ and $CuInSe_2$ chalcopyrites. The main reason may be such that the effective potential for the valence and conduction electrons in larger atom numbers becomes weaker because the greater atom number means the larger number of core electrons.[23–25] This leads to the fact that the ionization energy of the conduction electrons for the heavier atom in the same group of the periodic table of elements is smaller.[23] Thus, the phase transition occurs under a relatively lower pressure.

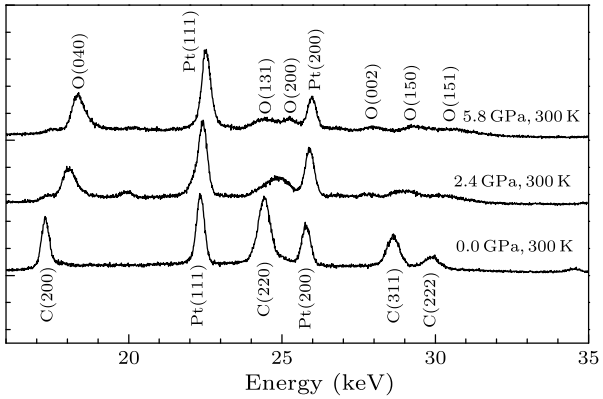

Fig. 1. Energy dispersive x-ray diffraction patterns of galena under the $P-T$ conditions indicated. C: cubic structure peak, O: orthorhombic structure peak.

Table 2. The experimental transition pressure of PbS.

Sample	NaCl-TlI-type (GPa)	References
PbS	2.2	[7]
PbS	2.5	[8]
$Pb_{0.99}S_{1.01}$	2.4	This study

As the data of NaCl type is too few, we fit only the data of the TlI-type phase. Using the Pt scale of Holmes *et al.*[13] as a reference pressure scale, we obtain the $P-V$ data of TlI-type phase for galena (Table 1). These room-temperature data are fitted using the third-order Birch–Murnaghan EOS:

$$P = \frac{3}{2}K_0\left[\left(\frac{V_0}{V}\right)^{7/3} - \left(\frac{V_0}{V}\right)^{5/3}\right] \times \left\{1 + \frac{3}{4}(K_0' - 4)\left[\left(\frac{V_0}{V}\right)^{2/3} - 1\right]\right\}, \quad (1)$$

where V_0, K_0, K_0' are the zero-pressure volume, isothermal bulk modulus and its pressure derivative, respectively. The experimental $P-V$ data are fitted to the Birch–Murnaghan EOS. The fits yield $V_0 = 197(2)\,\text{Å}^3$, $K_0 = 37(5)\,\text{GPa}$, $K_0' = 3.5(8)$ (Fig. 3).

To assess the quality of fitting of the Birch–Murnaghan equation of state, obtained from the plot of unit cell volume against pressure, the relationship between the Eulerian strain ($f = 0.5[(V_0/V)^{2/3} - 1]$) and the normalized pressure ($F = P/[3f(2f+1)^{5/2}]$) is shown in Fig. 4. The $f-F$ plot provides a visual indication, of which higher order terms such as K_0' and K_0'' are significant in the equation of state. The fairly negative slope is obtained from the linear fit of the $f-F$ plot for the unit-cell volumes, in good agreement with the K_0' value smaller than 4 given by the Birch–Murnaghan EOS fit.

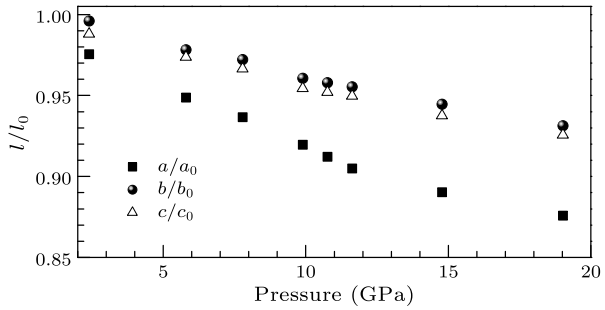

Fig. 2. Pressure dependences of relative cell parameters for TlI type.

The axial compressibilities of TlI type at room temperature, a/a_0, b/b_0 and c/c_0, are plotted as a function of pressure in Fig. 2. From Fig. 2, there appears to be a very slight discontinuity at 11 and 14 GPa. There is a possible source for this phenomenon in which we use a methanol-ethanol-water mixture with 16 : 3 : 1 for the pressure medium, which freezes above 10 GPa, and the hydrostatic circumastance of sample chamber will be influenced.

Unit cell parameters of TlI type at room temperature are fitted using a form of the third-order finite strain (Birch–Murnaghan) equation modified for axial compression:[26,27]

$$P = \frac{3}{2}K_{l0}\left[\left(\frac{l_0}{l}\right)^{7/3} - \left(\frac{l_0}{l}\right)^{5/3}\right] \times \left\{1 + \frac{3}{4}(K_{l0}' - 4)\left[\left(\frac{l_0}{l}\right)^{2/3} - 1\right]\right\}, \quad (2)$$

where K_{l0} and K_{l0}' are the zero-pressure incompressibility and pressure derivative of the l-axis ($l = a$, b, c). From fits to the experimental data, the values of a_0, b_0, and c_0 obtained at ambient P are 4.11(4) Å, 11.29(5) Å, and 4.16(2) Å, respectively. The zero-pressure axial compressibility β_l has the form[26,27]

$$\beta_l = 1/(3K_l). \quad (3)$$

Assuming a linear relationship between these parameters and pressures, we obtain the mean axial compressibilities of a-, b- and c-axes to be $3.4 \times 10^{-3}\,\text{GPa}^{-1}$, $1.4 \times 10^{-3}\,\text{GPa}^{-1}$ and $1.6 \times 10^{-3}\,\text{GPa}^{-1}$, respectively. The compressibility of TlI type is the largest along the a unit-cell edge and the least along the b unit-cell edge.

The high-temperature data of TlI type are fitted to the high-temperature Birch–Murnaghan equation of state (Fig. 5). Because of the lower experimental temperature, we assume that the second- and higher-order pressure derivatives of the bulk modulus are negligible in this study, i.e. bulk modulus K is linearly dependent on temperature. Then K_T and K_0 are given by the properties under ambient conditions,

$$K_T = K_0 + (\partial K/\partial T)_P(T - 300), \quad (4)$$

where $(\partial K/\partial T)_P$ is the temperature derivative of the bulk modulus.

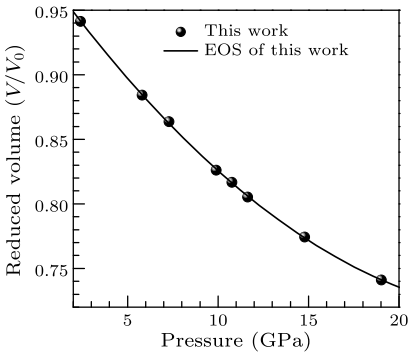

Fig. 3. Isothermal equation of state of TlI type. Solid curve: the Birch–Murnaghan equation fit with K_0 and K_0' being 37 GPa and 3.5, respectively. The size of the symbols exceeds the uncertainties.

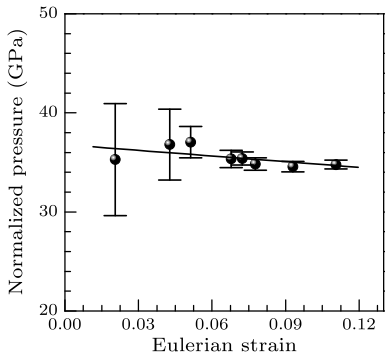

Fig. 4. Eulerian strain-normalized pressure ($f-F$) plot of the TlI-type data based on the Birch–Murnaghan equation of state. The solid line represents the linear fit.

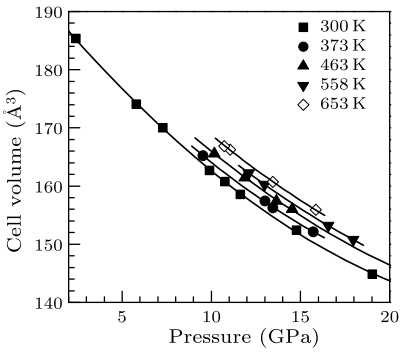

Fig. 5. $P-V-T$ relations of TlI type. Solid curves are for the isothermal compression calculated by the best fitting parameters; $K_0 = 37(3)\,\text{GPa}$, $K_0' = 3.6(3)$, $(\partial K/\partial T)_P = -0.022(9)\,\text{GPaK}^{-1}$, and $\alpha_0 = 2.2(5) \times 10^{-5}\,\text{K}^{-1}$.

Table 3. The thermoelastic parameters for TlI-type of PbS. The numbers in parentheses are uncertainties on the last digits.

Sample	Method	K_0(GPa)	K_0'	$(\partial K/\partial T)_P$ (GPaK^{-1})	α_0 (10^{-5} K^{-1})	References
PbS	Experiment	30.9(4)	4(fixed)			[8]
PbS	Calculation	34.0	4.8			[10]
PbSe	Calculation	31.0	4.9			[10]
PbTe	Calculation	27.0	4.9			[10]
$Pb_{0.99}S_{1.01}$	Experiment	37(5)	3.5(8)			This study (PV)
$Pb_{0.99}S_{1.01}$	Experiment	37(3)	3.6(3)	−0.022(9)	2.2(5)	This study (PVT)

The temperature effect for V_T is expressed as

$$V_T = V_0 \exp \int_{300}^{T} \alpha_T dT, \tag{5}$$

where α_T is the volume thermal expansivity coefficient and at ambient pressure it is expressed as a linear function of temperature

$$\alpha_T = \alpha_0 + \alpha_1 T. \tag{6}$$

Substituting Eqs. (4) and (6) into Eq. (1), we obtain $V_0 = 197(1)\,\text{Å}^3$, $K_0 = 37(3)\,\text{GPa}$, $K_0' = 3.6(3)$, $(\partial K/\partial T)_P = -0.022(9)\,\text{GPaK}^{-1}$, $\alpha_0 = 2.2(5) \times 10^{-5}\,\text{K}^{-1}$ (Fig. 5).

The bulk moduli obtained by the two approaches (PV and PVT EOS) are in good agreement with each other, and slightly larger than those in the previous studies (Table 3). From Table 3, we can find that the value of K_0' in this study is smaller than the previous studies. The K_0' value would increase the static compression K_0 value of this study, because the calculated K_0 value decreases with increasing K_0'.[28] Thus we infer that the smaller K_0' is the main reason for the relatively larger bulk modulus in this study.

In addition, comparing the bulk moduli for the TlI type of PbS, PbSe and PbTe, we observe that the bulk moduli reduce in turn with the increasing atomic number in anion (Table 3). There are two possible sources for this situation. First, the ionic radii of S, Se and Te increase [$S^{2-}(1.84\,\text{Å}) < Se^{2-}(1.91\,\text{Å}) < Te^{2-}(2.11\,\text{Å})$]. Second, the electronegativities of S, Se and Te decrease (S = 2.58 < Se = 2.55 < Te = 2.1). Electronegativity is a chemical property that describes the ability of an atom to attract electrons. An atom's electronegativity is affected by its atomic weight and the distance of its valence electrons from the charged nucleus. The higher the associated electronegativity number, the greater an element or compound attracts electrons.[29] The inoic radius and electronegativity may have a significant influence on bulk modulus.[30] The larger the inoic radius and electronegativity, the stronger the attraction for the bonding electron, and the greater the electron density between cation and anion, resulting in the fact that crystals have greater compressed resisted capacity.[30] Therefore, we consider that the ionic radius and electronegativity are the main reasons for the bulk moduli reduce in turn with the increasing atomic number in anion for TlI type of PbS, PbSe and PbTe.

In summary, the phase relations and compression behavior of galena ($Pb_{0.99}S_{1.01}$) at pressures up to 19.0 GPa in the temperature range 300–653 K have been obtained using the exterior heating DAC technique. The phase transition from NaCl type to TlI type takes place at approximately 2.4 GPa. The temperature derivative of the bulk modulus $(\partial K/\partial T)_P$ and the thermal expansivity coefficient for TlI type of galena are obtained for the first time. Furthermore, we confirm that the linear compressibilities β along a, b and c directions of TlI type is elastically anisotropic ($\beta_a = 3.4 \times 10^{-3}\,\text{GPa}^{-1}$, $\beta_b = 1.4 \times 10^{-4}\,\text{GPa}^{-1}$ and $\beta_c = 1.6 \times 10^{-3}\,\text{GPa}^{-1}$), with the a-axis exceeding twice as compressible as the b- and c-axes.

References

[1] Tang L Y et al 2010 *Chin. Phys. Lett.* **27** 016402
[2] Ma Y M et al 2007 *Chin. Phys. Lett.* **24** 1180
[3] Runge C E et al 2006 *Phys. Chem. Miner.* **33** 699
[4] Qin S et al 2003 *Chin. Phys. Lett.* **20** 1172
[5] Zhang W W et al 2002 *Chin. Phys. Lett.* **19** 1666
[6] Samara G and Drichamer H G 1962 *J. Phys. Chem. Solids* **23** 457
[7] Chattopadhyay T et al 1986 *Physica* B **139/140** 356
[8] Knorr K, Ehm L, Hytha M, Winkler B and Depmeier W 2003 *Eur. Phys. J.* B **31** 297
[9] Grzechnik A and Friese K 2010 *J. Phys.: Conden. Matter* **22** 095402
[10] Ahuja R 2003 *Phys. Status Solidi* B **235** 341
[11] Qadri S B, Yang J, Ratna B R, Skelton E F and Hu J Z 1996 *Appl. Phys. Lett.* **69** 2205
[12] Jiang J Z et al 2000 *J. Appl. Phys.* **87** 2658
[13] Holmes N C et al 1989 *J. Appl. Phys.* **66** 2962
[14] Liu J, Zhao J, Che R Z and Yang Y 2000 *Chin. J. High Pressure Phys.* **14** 247 (in Chinese)
[15] Jiang X, Zhou W G, Xie H S, Liu Y G, Fan D W, Liu J, Li Y C, Luo C J and Ma M N 2007 *Chin. Phys. Lett.* **24** 287
[16] Yu S C, Spain I L and Skelton E F 1978 *Solid State Commun.* **25** 49
[17] Itkin G, Hearne G R, Sterer E, Pasternak M P and Potzel W 1995 *Phys. Rev.* B **51** 3195
[18] Strössner K, Ves S, Kim C K and Cardona M 1987 *Solid State Commun.* **61** 275
[19] Fan D W, Zhou W G, Liu C Q, Wan F, Xing Y S, Liu J, Li Y C and Xie H S 2009 *Chin. Phys. Lett.* **26** 046402
[20] Ohtani A, Seike T, Motobayashi M and Onodera A 1982 *J. Phys. Chem. Solids* **43** 627
[21] Kumar R S, Sekar A, Jaya N V, Natarajan S and Chichibu S 2000 *J. Alloys Compd* **312** 4
[22] Tinoco T, Polian A, Gomez D and Itie J P 1996 *Physica Status Solidi* B **198** 433
[23] Hao A M, Gao C X, Li M, He C Y, Huang X W, Zhang D M, Yu C L, Liu H W, Ma Y Z, Tian Y J and Zou G T 2007 *J. Phys.: Conden. Matter* **19** 425222
[24] Philips J C and Kleinman L 1959 *Phys. Rev.* **116** 287
[25] Cohen M N and Heine V 1961 *Phys. Rev.* **122** 1821
[26] Xia X, Werdner D J and Zhao H 1998 *Am. Mineral.* **83** 68
[27] Angel R J 2000 *Rev. Mineral. Geochem.* **41** 35
[28] Nishihara Y, Takahashi E, Matsukage K and Kikegawa T 2003 *Am. Mineral.* **88** 80
[29] Allen L C 1989 *J. Am. Chem. Soc.* **111** 9003
[30] Zhang J 1999 *Phys. Chem. Miner.* **26** 644